

See discussions, stats, and author profiles for this publication at: <https://www.researchgate.net/publication/274387208>

Geochemistry and petrology of palaeocene coals from Spitzbergen — Part 2: Maturity variations and implications for local and regional burial models

Article in *International Journal of Coal Geology* · March 2015

Impact Factor: 3.38 · DOI: 10.1016/j.coal.2015.03.013

CITATIONS

3

READS

72

10 authors, including:



Will Meredith

University of Nottingham

59 PUBLICATIONS 976 CITATIONS

SEE PROFILE



Christopher H Vane

British Geological Survey

91 PUBLICATIONS 1,375 CITATIONS

SEE PROFILE



Baruch Spiro

Natural History Museum, London

176 PUBLICATIONS 4,117 CITATIONS

SEE PROFILE



Colin E. Snape

University of Nottingham

462 PUBLICATIONS 8,039 CITATIONS

SEE PROFILE

1 **Maturity Issues within Palaeocene Coal, Spitsbergen: Implications for local**
2 **and regional burial and uplift models**

3
4 Chris Marshall^{a*}, Jacob Uguna^a, David J. Large^a, Will Meredith^a, Malte Jochmann^b,
5 Bjarki Friis^b, Christopher H. Vane^c, Baruch F. Spiro^d, Colin E. Snape^a, Alv Orheim^e

6 ^{a*}Corresponding Author; Christopher.Marshall@nottingham.ac.uk Department of Chemical and
7 Environmental Engineering, Faculty of Engineering, University of Nottingham, University Park,
8 Nottingham NG7 2RD, UK (0115) 9514114

9 ^bStore Norske AS, PO Box 613, NO-9171 Longyearbyen, Norway

10 ^c British Geological Survey, Nicker Hill, Keyworth, Nottingham, NG12 5GG, UK

11 ^dDepartment of Mineralogy, Natural History Museum, Cromwell Road, London SW7 5BD, UK

12 ^e GeoArktis As, Rosestien 3, N-4022 Stavanger, Norway

13
14 **The Central Tertiary Basin is an uplifted part of the North Barents Shelf and**
15 **should be an ideal location to understand the thermal history, maximum**
16 **burial depth and overburden thickness in this petroleum-rich area. Efforts to**
17 **quantify the thermal history of the region have been hampered by reports of**
18 **hyper-thermal conditions, maturity gaps and maturity inversions in the**
19 **Tertiary vitrinite reflectance (R_o) record. This has been attributed to thermal**
20 **insulation effects, bitumen suppression and later Tertiary volcanism.**
21 **Through the use of R_o , organic maturity parameters, ^{13}C NMR and Rock-Eval**
22 **pyrolysis, this study aims to explain the unusual maturity effects observed and**
23 **the implications for burial models. Within single seams, R_o % ranges from 0.5-**
24 **0.78 with increasingly bimodal distribution up-seam. Analysis of coal**
25 **aromaticity and the results of Rock-Eval analysis confirm that maturity gaps**
26 **and inversions only occur where the vitrinite reflectance has been suppressed**
27 **by high bitumen content (300-400 mg/g coal). Samples with the lowest**
28 **hydrogen index values (<250 mg HC/ TOC) provide the most accurate estimates**
29 **of the vitrinite reflectance. Results indicate maximum burial temperatures of**
30 **120°C in the basin centre and 100°C at the basin margins with a hyper-thermal**
31 **gradient of approximately 50°C/km. This gradient implies a total overburden**
32 **of 2 km of which 1 km has been lost. Maximum burial depth and total**
33 **erosional sediment load to the Barents Shelf are therefore at the lower end of**
34 **current estimates.**

35

36 **Key Words**

37 Vitrinite Reflectance, Oil prone coal, Maturity, Barent Shelf, Spitsbergen

38 **1. Introduction**

39 Apparent maturity gaps and maturity inversions in vitrinite reflectance (R_o) data
40 appear common within the Central Tertiary Basin, notably between the Triassic-
41 Jurrassic boundary and Cretaceous-Basal Tertiary strata_(Paech and Koch, 2001).
42 Orheim et al. (2007) also report a maturity gap (R_o %=0.94 vs. 0.71) within Basal
43 Tertiary Firkanten Formation coal seams which stratigraphically are only 40 m apart.
44 Tertiary vitrinite reflectance (R_o) data forms a key part of many estimates regarding
45 geothermal gradient, maximum burial depth and overburden loss (Major and Nagy,
46 1972, Manum and Throndsen, 1978, Throndsen, 1982, Paech and Koch, 2001). Any
47 significant suppression of vitrinite may therefore lead to changes to estimates of erosion
48 and transportation to local depocentres such as the Barents Sea,

49 Orheim et al., (2007) provide two possible explanations for apparent maturity variations
50 within the Tertiary coals, namely the insulation effect of an underlying seam and
51 suppression of vitrinite reflectance by bitumen enrichment. Hyper-thermal conditions
52 during burial have been implied in a number of studies of the Adventdalen Area (Fig. 1;
53 Major and Nagy, 1972, Manum and Throndsen, 1978, Throndsen, 1982, Paech and
54 Koch, 2001, Braathen, 2012). In addition, it is clear that the Central Tertiary Basin was
55 subject to local volcanic activity during the Tertiary as shown by numerous bentonite
56 beds in Van Mijenfjorden Group sediments (Fig. 2), and a dolerite sill in the
57 Bjørndalen/Fuglefjellet region_(Pers. Comm. Trygvason Eliassen, 2014). The effect on
58 vitrinite reflectance in the case of intrusions is expected to be significant but highly
59 localised.

60 Vitrinite suppression by bitumen is well documented in oil source rocks including coals.
61 Fluorescent (perhydrous) vitrinites enriched in hydrogen rich material are an indicator
62 of oil potential and therefore of the potential for suppressed vitrinite reflectance (R_o)
63 values (Diessel and Gammidge, 1998). As vitrinite reflectance is an indirect measure of
64 aromaticity (Carr and Williamson, 1990) any excess aliphatic material will lead to R_o
65 values suppression. Orheim et al. (2007) observed that the upper Firkanten formation
66 coals fluoresce under UV light and produce droplets of oil during preparation. In
67 addition, Marshall (2013) show that the coals produce up to 40 wt% hydrocarbons, when

68 processed by Soxhlet solvent extraction and hydrous pyrolysis. This would indicate that
69 the coals have at least some oil potential and therefore bitumen suppression may
70 present a reasonable explanation.

71 In this study we examine bulk and high resolution vitrinite reflectance measurements to
72 examine whether reported R_o variability can be replicated. We utilise other independent
73 maturity parameters such as organic biomarkers, Rock-Eval and aromaticity to provide
74 an alternative measure of maturity in the coals. Focussing upon the role of oil potential
75 in R_o suppression we compare Rock-Eval hydrogen index (HI) values with vitrinite
76 reflectance to attempt to correct for the suppression effect. The implications for the
77 thermal regime, missing overburden estimates, sediment compaction and sediment
78 transportation to the Barents Sea are then discussed.

79 **2. Geological Setting**

80 Svalbard (Fig.1) represents an uplifted part of the Northern Barents shelf (Harland et
81 al., 1997) comprising Caledonian basement and subsequent uncomformable basin infill.
82 Much of central and southern Spitsbergen forms part of the Central Tertiary Basin a
83 asymmetric synclinal basin, bounded to the east and west by the Billefjorden Faultzone
84 and West Spitsbergen fold and thrust belt. Formed in response to the onset of
85 compression related West Spitsbergen foreland fold and thrusting and prior to the
86 strike-slip separation of Svalbard and Barents Shelf from Greenland (Harland, 1997,
87 Tessensohn, 2001) the Central Tertiary Basin contains sediments dating from as early
88 as the Carboniferous including many source rock analogues from the wider Barents sea
89 region. It also contains the majority of the economic coal deposits on the islands, with
90 mining concentrated within the Tertiary Firkanten Formation

91 In the NE Central Tertiary Basin, the Firkanten Formation comprises two sub-units;
92 the lowermost Todalen Member and the overlying Endalen Member representing a
93 sequence of paralic coalbearing tidal sediments overlain by laminated or heavily bio-
94 turbated marine sandstones (Fig. 2; Dallmann *et al.*, 1999). The base of the Firkanten
95 Formation is marked by a low angle unconformity with the Lower Cretaceous
96 Carlinefjellet formation, sometimes marked by a basal conglomerate known as the
97 Grønfjorden bed (Harland, 1997, Dallmann, 1999).

98

99 To the west an additional offshore unit is also observed, known as the Kolthoffberget
100 Member (Fig. 2; Dallmann, 1999). The Todalen Member represents the main coal

101 bearing unit within the Van Mijenfjorden Group and therefore is the focus of this study.
102 It consists of 3-5 siltstone-sandstone-coal successions representing increased subsidence
103 and the infilling of the Cretaceous pene-plain (Harland, 1997, Dallmann, 1999). Five
104 main coal seams are commonly cited within the Todalen Member; the Svea, Todalen,
105 Longyear, Svarteper and Askeladden Seams (Fig. 2; Dallmann, 1999, Harland, 1997,
106 Orheim et al., 2007)).

107

108 3. Methodology

109 Coal was sampled (Fig. 1) from the Svea Nord, Longyear and Svarteper seams from
110 mine sections in Svea Nord and Mine 7, boreholes from the Lunckefjellet (BH6A-2007,
111 BH10/2007, BH10/2009, BH15/2011), Adventdalen (BH4/2009, BH5/2009) and
112 Colesdalen (BH3/2008) regions, and a field section from Bassen. Samples were coarse-
113 crushed, separated by cone and quarter (to allow unbiased sampling for coal maceral
114 analysis) and the remainder fine crushed (<100 μm). Polished blocks (particle size; 0.2 –
115 1 mm) were created for organic petrology and vitrinite reflectance (R_o).

116

117 Coal vitrinite reflectance (R_o) was determined using a microscope fitted with a 50x oil
118 immersion objective and 10x oculars, 12 V 100 W quartz halogen lamp and 100 W HBO
119 high pressure mercury lamp. R_o measurements were taken using an attached
120 photomultiplier (100 points) and calibrated using a 1.24 R_o , 564 nm glass prisma
121 standard and blank plastic oil-filled depression according to BSI standards (British
122 Standard Institution, 2009).

123

124 To determine the amount of hydrocarbon potential the coals were analysed using a
125 Rock-Eval6 analyser configured in standard mode (pyrolysis and oxidation as a serial
126 process) to indicate the coals (20 mg dry wt) were heated from 300°C to 650°C at
127 25°C/min in an inert atmosphere of N_2 and the residual carbon then oxidised at 300°C to
128 850°C at 20°C/min (hold 5 min). Hydrocarbons released during the two stage pyrolysis
129 were measured using a flame ionization detector and CO and CO_2 measured using an IR
130 cell. The performance of the instrument was checked every 10 samples against the
131 accepted values of the Institut Français du Pétrole (IFP) standard (IFP 160 000, S/N1 5-
132 081840). Classical Rock-Eval parameters were calculated by integration of the amounts
133 of HC (thermo-vaporized free hydrocarbons) expressed in mg/HC/g rock (S_1) and
134 hydrocarbons released from cracking of bound OM expressed in mg/HC/g rock (S_2)

135 (Engelhart et al., 2013). The Hydrogen Index (HI) was calculated from $S_2 \times 100/\text{TOC}$ and
136 the Oxygen Index (OI), $S_3 \times 100/\text{TOC}$. The error on the T_{max} is about ± 6 °C.

137

138 In order to examine organic maturity parameters in the solvent extractable hydrocarbon
139 fraction from the Adventdalen coals (BH-5-2009 and Mine 7 Section), the coals were
140 subjected to accelerated solvent extraction (ASE) using a 93:7 DCM: methanol mixture
141 for a period of 24hrs, and separated into aliphatic, aromatic and polar fractions by silica-
142 alumina adsorption column chromatography (15 ml *n*-hexane; 15 ml *n*-hexane:DCM (3:2
143 v/v); 15 ml DCM:,methanol (1:1 v/v). Aliphatic and aromatic fractions were analysed by
144 GC-MS in both the SIM and full scan (m/z 50-450) modes, using a Varian CP-3800 gas
145 chromatograph, interfaced to a Varian 1200 mass spectrometer (EI mode, 70eV).
146 Separation was achieved on a VF-1MS fused silica capillary column (50m x 0.32 mm i.d,
147 0.25 μm stationary phase thickness), with helium as the carrier gas, and an oven
148 programme of 50°C (hold for 2 min) to 300°C (hold for 20.5 min) at a heating rate of
149 4°C/min. The m/z 85 single ion chromatogram (SIC) was used to measure *n*-alkane peak
150 area response. Relative hopane and sterane concentrations were from peak area
151 responses in the m/z 191 and m/z 217 SICs, respectively. MPI-1 was calculated from
152 the aromatic fraction from peak area responses from the m/z 178 and m/z 192 SICs
153 | respectively (after Cassani et al., 1988).

154

155 The ratio of aliphatic to aromatic components was determined in selected Svea Nord and
156 Longyear coal samples (1.20 m and 1.30 m above seam base respectively) using high
157 resolution solid state 50 MHz ^{13}C NMR. Analysis was carried out in a BrukerAvance
158 200 spectrometer to ascertain using the cross polarisation (CP) sequence in conjunction
159 with magic angle spinning (MAS). For CP-MAS analysis, the acquisition time was 0.05
160 s, the relaxation delay was 1.5 s and the contact time was 1 ms. Samples were packed
161 tight into a cylindrical (7 mm o.d.) zirconia rotor with a cap made of a homopolymer of
162 chlorotrifluoroethene (Kel-F) and spun at the magic angle (54.74°) with a spinning rate
163 of approximately 5 kHz. Tetrakis-trimethylsilyl silane (TKS) was added to the samples
164 as an internal standard. The number of scans was 2500 and the free induction decays
165 (FIDs) were processed using a line broadening factor of 50 Hz.

166

167

168

169

170 4. Results

171 4.1 Vitrinite Reflectance

172 Examination of vitrinite reflectance values (Table 1) from two bulk samples of Svea and
173 Longyear coal examined replicate the maturity gap reported by Orheim et al. (2007)
174 with R_o % values of 0.65 vs 0.78. Consequently, to understand how widespread and the
175 main cause of this difference in maturity the Longyear seam was examined at higher
176 resolution in coals from three sub-regions; Adventdalen, Lunckefjellet and Colesdalen.

177 4.2 Adventdalen

178 Coals from the Adventdalen region are vitrinite dominated with low inertinite and
179 liptinite with the exception of the Svea seam which is inertinite dominated. Vitrinites
180 are observed to exhibit dull orange/brown fluorescence under blue light. R_o values range
181 from 0.5-0.8 with the Svea seam showing generally highest values and uppermost
182 Longyear seam the lowest (Fig 3; Table S1). All sites show a similar range of R_o values
183 which is unexpected as the Bassen section is up-dip of samples from Breinosa area. The
184 distribution of R_o values exhibits the greatest range in Mine 7 and Bassen samples with
185 minimum values at Mine 7 of 0.5. There are distinct differences between upper and
186 lower seams in Mine 7 and Bassen section. These numerous small and large scale
187 variations comprising rapid R_o drops and inversions are unlikely to be the product of
188 differing thermal histories. Conversely R_o values from the BH4/2009 sample locality
189 remain consistently low, which is perhaps the product of a more homogenous
190 composition.

191 When the distribution of R_o data in the Mine 7 section is examined in greater detail it
192 indicates a general broadening of R_o measurements up-seam (Fig. 4) accompanied by a
193 gradual reduction in the number of higher reflectance measurements. In addition
194 rather than a single main peak, measurements become increasingly bimodal up-seam.
195 This bi-modality is possibly the product of variation in the relative number of
196 fluorescent vs. non-fluorescent vitrinites.

197 4.3 Lunckefjellet

198 The Lunckefjellet Longyear seam is vitrinite dominated (as in Adventdalen) with low
199 inertinite and liptinite. Vitrinites again exhibit dull orange/brown fluoresce under blue
200 light. Highest vitrinite reflectance values (≈ 0.76) are found towards the eastern margin

201 of the basin (Fig 5; Table S1) with decreasing R_o down dip which is contrary to
202 expectations. In addition the Longyear seams exhibit a general decrease in R_o up-seam
203 similar to that seen in Adventdalen. The greatest range of R_o values (Fig. 5) can be found
204 in the easternmost sampling locality's with values ranging from R_o % 0.59-0.76. These
205 numerous small and large scale variations comprising rapid R_o drops and inversions are
206 unlikely to be the product of differing thermal histories. As in Adventdalen, when the
207 distribution of R_o data in the Lunckefjellet section (Fig. 6) is examined in greater detail
208 it indicates a general broadening of R_o measurements up-seam (Fig 6). In addition
209 measurements become increasingly bimodal up-seam. The high degree of similarity
210 between the Adventdalen and Lunckefjellet coals indicates that a similar process is
211 controlling the large variations in vitrinite reflectance at both sites.

212 4.4 Colesdalen

213 The Colesdalen coals are higher in inertinite (compared to the other coals in this study)
214 but still vitrinite dominated. The Colesdalen coals have elevated R_o values (0.78) as
215 expected from a more central part of basin (Table S1). In addition the Colesdalen coals
216 show less variability with values consistently high throughout the seam with the
217 exception of two more ash rich samples.

218 The vitrinite reflectance measurements (Table S1) from the Lunckefjellet and
219 Adventdalen regions show large variations (R_o % \approx 0.3) within some parts of the seam
220 and importantly replicate the maturity gap observed (Orheim et al., 2007). These
221 numerous small and large scale variations comprising rapid R_o drops and inversions are
222 unlikely to be the product of differing thermal histories. As a result, the suitability of
223 vitrinite reflectance in these coals as a measure of maturity will be examined by
224 comparing R_o data with independent measures of maturity such as organic maturity
225 parameters, Rock-Eval and aromaticity.

226 4.5 Organic Maturity parameters

227 Coals from BH 5/2009 and Mine 7 were selected to further examine the true maturity of
228 the Svea, Longyear and Svarteper seams through organic geochemical biomarkers in
229 Soxhlet extracted oils. Organic Geochemical maturity parameters (Table 1) can be
230 highly specific at low maturities but often reach equilibrium at around R_o 0.7%, making
231 many of little use at higher maturities (Peters et al., 2005).

232 Aliphatic maturity parameters for the Todalen coals are at or approaching equilibrium
233 (Table. 1) indicating a maturity in excess of R_o 0.7%. The *n*-alkanes show little odd over
234 even predominance, with carbon preference index values (CPI(1),(Bray and Evans,
235 1961)) close to mature ratios (≈ 1). Notably, both CPI(1), sterane and hopane maturity
236 parameters shown no change up-seam in the Longyear (Fig.7) contrary to what would be
237 expected if R_o values at the top of the seam represented true maturity values and were
238 not suppressed.

239 Consideration of the aromatic Methylphenanthrene Index, MPI-1 (Radke et al., 1982,
240 Radke et al., 1986, Radke, 1988) predicts R_o values of around 0.72 ± 0.05 in the Svea,
241 Longyear and Svarteper seams in the Adventdalen region with no changes up-seam
242 (Table 1). Although the predicted values are lower than maximum R_o values measured
243 in these coals ($R_o \% \approx 0.78$), the predicted values remain substantially higher than the
244 lowest values measured at the top of the Longyear seam in Mine 7 ($R_o \% \approx 0.5$). A
245 possible explanation for the difference is the effect of variation in organic matter source
246 and migration (Peters et al., 2005). Differences between predicted MPI-1 R_o % (0.72)
247 and measured R_o (0.79) in the Svea seam at both Adventdalen and Svea Nord are likely
248 a product of differing palaeo-environment and associated organic matter.

249 In summary, geochemical evidence points to both seams having comparable maturities
250 and thermal histories. Significantly, the R_o maturity gap, both within the Longyear
251 seam and between the Svea and Longyear seams is not reproduced geochemically.

252 **4.6 Oil Potential and Maturity**

253 T_{max} , like many maturity parameters is highly dependent upon source material (Peters
254 et al., 2005) but is considered of use for assessment of Type II material (420-460°C) and
255 Type III (400-600°C; Tissot et al., 1987). T_{max} ranges from 425–448°C for all the
256 Svalbard coals indicating a maximum maturity in the early-mid oil window (Table. S2).
257 When T_{max} is plotted against HI (indicative of source rock potential; Fig. 8) there is a
258 general positive correlation with coal from the basin margin at Lunckefjellet and Bassen
259 least mature and Colesdalen coals from the basin centre more mature. HI also appears
260 to peak within the coals between T_{max} values between 435 and 445°C. This is similar to
261 the HI_{max} concept, and is associated with the reorganisation of kerogen structure
262 (Petersen, 2005).

263 | When T_{\max} is converted to R_o (Teichmüller and Durand, 1983) values were elevated
264 | compared to measured values indicating thermal maturity R_o % ≈ 0.83 (Table S2) for all
265 | samples in the Adventdalen region with the exception of Bassen where the more
266 | marginal basin setting means the coals are inherently less mature. Coals from the Svea
267 | Nord seam are slightly more mature than those in Adventdalen, consistent with the
268 | southward tilting of the Central Tertiary Basin. The Svea Nord seam has values around
269 | 0.85. The Lunckefjellet coals appear less mature than the Svea Nord and Adventdalen
270 | coals with calculated R_o % values of 0.66, perhaps consistent with a more marginal
271 | setting. The Colesdalen coals as expected due to their more central location are more
272 | mature with calculated R_o % values of 0.83.

273 | The production index ($PI = S_1/(S_1+S_2)$) is another indicator of maturity values, < 0.1
274 | indicate an immature source rock and values > 0.4 , a mature source rock (Maky and
275 | Ramadan, 2008). The Svalbard coals all have values < 0.1 (Table. S2; Fig 8), suggesting
276 | the coals were exhumed prior to any significant generation of hydrocarbons, with
277 | Colesdalen the most mature with values approaching 0.1 (Fig.8). As with T_{\max} the coals
278 | with the highest HI values appear to be closest to generation, particularly in the
279 | Colesdalen region (Fig.8). The Bassen region appears to have unusually low free
280 | hydrocarbon values which may reflect weathering at the field site. Values of T_{\max}
281 | appear slightly high compared to PI values which indicate that the coals are sub-
282 | mature. This may be due to the extended oil window in coals compared to other
283 | conventional source rocks (Petersen and Nytoft, 2006).

284 | HI values in the Svea seam are generally < 250 mg HC/TOC with upper seams ranging
285 | between 250-400 mg HC/TOC (Table S2). This confirms that the upper coal seams
286 | across eastern central basin have significant oil potential compared to the Svea Seam.
287 | The plot of HI vs OI (Fig.8) shows that most samples have compositions between that of
288 | Type II and Type III kerogen. OI is elevated and HI lower in the Bassen area indicates
289 | either lower maturity or weathering of samples. As this is a field sample and the
290 | vitrinite reflectance variations are similar to other sample locations in the area it is
291 | thought most likely to indicate weathering.

292 | Examination of the relationship between HI and R_o (Fig.8) shows that all sites show
293 | strong negative correlation between R_o and HI indicating that the higher the oil
294 | potential the more suppressed vitrinite becomes. However the different gradients and
295 | positions of these lines show that this relationship is complicated by other factors.
296 | These are likely to be compositional, positional and weathering effects. This indicates

297 that samples with the lowest HI values provide a better reflection of the degree of
298 coalification ($\approx R_o$ % 0.78-0.80). This fits better with the production and migration of
299 hydrocarbons described previously (Orheim et al., 2007, Marshall, 2013). Consequently,
300 bitumen must have a suppressing effect on R_o across the basin.

301 **4.7 Quantifying the suppression effect**

302 Direct measurement of aromaticity (of which R_o is an indirect measurement) is a useful
303 tool in the derivation of maturity in some coals (Stephens et al., 1985, Carr and
304 Williamson, 1990).

305 The aromaticity (%) of the Svalbard coals (Fig.9) differs greatly between the Longyear
306 and Svea seams (50% vs. 70% respectively). Using the calibration of Carr and
307 Williamson, (1990), yields equivalent R_o values of 0.76 % (Svea) and 0.50% (Longyear).
308 This is clearly not the case, as the Longyear seam bears no resemblance to a brown coal
309 and is likely to have entered the early oil window in most areas. The Svea, which is not
310 oil prone, exhibits an aromaticity consistent with observed maturity. Consequently, the
311 observed maturity gap between the Svea and Longyear seams must be caused by
312 significant amounts of additional aliphatic material within the Longyear seam.

313 To quantify this suppression effect from normal bituminous Svea coal (75 parts
314 aromatic: 25 parts aliphatic), additional aliphatic carbon within the oil prone Longyear
315 coal would account for 33% of total carbon. This is approximately equivalent to 380-
316 400mg/g TOC, which is very close to HI values observed throughout the Eastern Central
317 Tertiary Basin (Table S2). Variations in the amount of additional aliphatic material
318 must therefore be responsible for apparent inter and intra seam maturity variation,
319 maturity gaps and maturity inversions within Firkanten Formation coals.

320 **5. Discussion**

321 **5.1 Maturity of coals**

322 At a bulk scale the R_o difference observed (Orheim et al., 2007) has been replicated with
323 the Longyear seam in particular appearing to show a rapid decrease in maturity up-
324 seam. However, this variability does not appear to be replicated by independent
325 measures of maturity such as organic maturity parameters and Rock-Eval. In addition
326 these parameters indicate that the coals have a thermal maturity in excess of R_o % 0.70
327 indicating that the coals reached maturities consistent with the early to mid oil window.

328 The bulk sample from the Longyear coal contains around 30% extra aliphatic material
 329 compared to the Svea seam. This is likely to reflect enrichment in bitumen. This liquid
 330 hydrocarbon potential is seen throughout the localities with Rock-Eval HI values
 331 ranging from 250-400mg HC/TOC. This is consistent with observed oil production
 332 (Orheim et al., 2007) and total hydrocarbon yields from Rock-Eval (300-400 mg
 333 HC/TOC) and Soxhlet/hydrous pyrolysis (300-400 mg/g HC; Marshall, 2013).

334 The effect upon R_o is clear (Fig.8) showing the higher HI values are the more suppressed
 335 R_o values become. This vitrinite suppression effect by the enrichment of later seams in
 336 aliphatic rich bitumen compared to non-oil prone Svea seams is therefore considered the
 337 primary cause for the maturity gaps and inversions observed by Orheim et al., (1997)
 338 (Orheim et al., 2007). Consequently, earlier Carboniferous, Jurassic and Cretaceous
 339 coals in the basin with observed coal rank inversion and maturity gaps (Paech and
 340 Koch, 2001) may benefit from further examination of this effect. The most accurate
 341 values for the Longyear seam appear to be found at the base of the seam which would
 342 give thermal maturities of the coals of R_o % of 0.78 at Breinosa, 0.68 at Bassen, 0.76 at
 343 Lunckefjellet and 0.80 in the Colesdalen area.

344 5.2 Thermal regime and implications for overburden models

345 Previous models measuring coalification gradients in Tertiary strata from the
 346 Adventdalen area range from between 0.17-0.32% R_o /km (Paech and Koch, 2001 and
 347 references therein). However due to the bitumen suppression effect it is likely that R_o
 348 values lie somewhat higher than previously thought. As the highest values of R_o in each
 349 seam appear the most reliable the maximum overburden and thermal regime at peak
 350 burial was calculated using these values and the empirical palaeo-temperature equation
 351 (Barker and Pawlewicz, 1994);

$$\text{Max T (}^\circ\text{C)} = \frac{\text{Ln}(R_o) + 1.68}{0.0124}$$

352 R_o values indicate estimated peak temps of 116°C in the Colesdalen area, 111°C at
 353 Breinosa, 110°C at Lunckefjellet and 100°C at Bassen. As expected, coals from the
 354 centre of the basin were exposed to the highest temperatures and vice versa. Given
 355 normal continental geothermal gradients (25°C/km) and assuming no other heat sources
 356 (Corcoran and Clayton, 1999) this would reflect maximum burial depths of 4.6 km, 4.4
 357 km, 4.4 km and 4.0 km respectively. In the Adventdalen area this would equate to a

358 total missing overburden of 3.4 km which is much greater than other estimates from the
359 Central basin (Paech and Koch, 2001 and references therein).

360 Assuming reported R_o values of 0.43 for the upper Tertiary coals from the Aspelintoppen
361 Formation are correct (Thronnsen, 1982) and values for the stratigraphically lower
362 Firkanten Formation coals 0.78 then the R_o gradient will be 0.35 R_o/km . This is
363 consistent with the highest previous estimates (Paech and Koch, 2001). When converted
364 using the Barker and Pawlewicz, 1994 equation this equates to a geothermal gradient of
365 around 50°C/km, similar to previous estimates (40°C/km; Braathen et al., 2012) and
366 maximum burial depths of 2.3km in the Colesdalen area, 2.2km at Breinosa, 2.2 km at
367 Lunckefjellet and 2.0 km at Bassen. As approximately 1.0 km of overlying strata still
368 exists in the Adventdalen Region (Thronnsen, 1982) the missing overburden is likely to
369 amount to ~1.0 km. This is lower than the values of 1.7km previously reported (Paech
370 and Koch, 2001 and references therein). In more central and southern areas of the
371 basin, accounting for vitrinite suppression, would also greatly reduce the current
372 estimated 3 km of eroded overburden (Manum and Thronnsen, 1978).

373 Previous studies support the conclusion (Major and Nagy, 1972, Manum and Thronnsen,
374 1978, Thronnsen, 1982, Paech and Koch, 2001) that the geothermal gradient during
375 burial was hyper-thermal. This is unsurprising as the Central Tertiary Basin was
376 formed during a period of both local and regional tectonic activity. Additionally the
377 presence of a dolerite sill in the Bjørndalen area (Pers. Comm. Trygvason Eliassen,
378 2014) and the numerous volcanic bentonites within Tertiary strata indicate volcanism
379 played an important role in shaping the thermal history of the Central Tertiary Basin.
380 Hyper-thermal conditions may also explain the relatively low levels of compaction
381 observed in Tertiary strata when compared to their apparent maturity.

382 Within a regional context, the Northern Barents including Svalbard (regarded as an
383 uplifted NW edge of the Barents Shelf, Harland, 1997) was subjected to less burial and
384 subsequent uplift and erosion than previously thought (Manum and Thronnsen, 1978,
385 Thronnsen, 1982, Paech and Koch, 2001) and consequently fits with lower estimates of
386 erosion and sediment load to the Southern Barents during the late Cenozoic (Rasmussen
387 and Fjeldskaar, 1996).

388

389

390 **6. Conclusions**

391 Inferred maturity gaps within the Svalbard coal are shown to be due to suppression of
 392 vitrinite reflectance by bitumen enrichment. Upper Firkanten formation coals have
 393 significant oil potential (HI 250-400mg HC/TOC), they appear most affected by maturity
 394 issues, displaying considerable variability in R_o values. Only the lowermost (and least oil
 395 prone) parts of the coal seams remain relatively unaffected. Using these values for the
 396 Adventdalen region, indicates R_o % values ranging from 0.68 at the basin margin to 0.78
 397 4 km down-dip, At Lunckefjellet R_o % values are around 0.76 and in the more centrally
 398 located Colesdalen values of 0.80. Coalification gradients in Adventdalen equate to
 399 $\sim 0.35 R_o/km$ consistent with highest previous estimates (Paech and Koch, 2001), a
 400 thermal gradient of approximately $50^\circ C/km$ and peak burial depths of $\sim 2km$ in the
 401 Adventdalen region. This indicates overall overburden erosion was less than previous
 402 estimates (1.7km; Manum and Throndsen, 1978) at around 1.0 km. The results of this
 403 study indicate that burial and subsequent uplift and erosion were perhaps lower than
 404 previously thought, leading to less compaction of tertiary strata on Svalbard and
 405 resulting in reduced sediment load to the Barents Shelf in the Late Tertiary.

406 **Acknowledgements**

407 We wish to thank Statoil & Store Norske AS for providing the samples used in this
 408 study. Many thanks also to Mr. David Clift for assistance with maceral analysis and
 409 sample preparation, Prof. Trevor Drage for assistance with NMR and Prof. Snorre
 410 Olausen and the University Centre on Svalbard for helpful discussions and logistical
 411 support. Financial Support by Store Norske AS/University of Nottingham studentship
 412 and NERC Studentship is gratefully acknowledged.

413 **References**

- 414 BARKER, C., E. & PAWLEWICZ, M., J. 1994. Calculation of Vitrinite Reflectance from
 415 Thermal Histories and Peak Temperatures. *Vitrinite Reflectance as a Maturity*
 416 *Parameter*. American Chemical Society.
- 417 BRAATHEN, A., BÆLUM, K., CHRISTIANSEN, H. H., DAHL, T., EIKEN, O.,
 418 ELVEBAKK, H., HANSEN, F., HANSEN, T. H., JOCHMANN, M.,
 419 JOHANSEN, T. A., JOHNSEN, H., LARSEN, L., LIE, T., MERTES, J., MØRK,
 420 A., MØRK, M. B., NEMEC, W., OLAUSSEN, S., OYE, V., RØD, K., TITLESTAD,
 421 G. O., TVERANGER, J. & VAGLE, K. 2012. The Longyearbyen CO₂ Lab of
 422 Svalbard, Norway - initial assessment of the geological conditions for CO₂
 423 sequestration. *Norwegian Journal of Geology*, 92, 353-976.

- 424 BRAY, E. E. & EVANS, E. D. 1961. DISTRIBUTION OF NORMAL-PARAFFINS AS A
 425 CLUE TO RECOGNITION OF SOURCE BEDS. *Geochimica Et Cosmochimica*
 426 *Acta*, 22, 2-15.
- 427 BRAY, R. J., GREEN, P. F. & DUDDY, I. R. 1992. Thermal history reconstruction using
 428 apatite fission track analysis and vitrinite reflectance: a case study from the UK
 429 East Midlands and southern North Sea. *In: HARDMAN, R. F. P. (ed.)*
 430 *Exploration Britain: geological insights for the next decade*. London: Geological
 431 Society of London.
- 432 BRITISH STANDARD INSTITUTION 2009. BS ISO 7404-5:2009: Methods for the
 433 petrographic analysis of coals –Part 5: Method of determining microscopically the
 434 reflectance of vitrinite. London: British Standard Institution.
- 435 CARR, A. D. & WILLIAMSON, J. E. 1990. THE RELATIONSHIP BETWEEN
 436 AROMATICITY, VITRINITE REFLECTANCE AND MACERAL COMPOSITION
 437 OF COALS - IMPLICATIONS FOR THE USE OF VITRINITE REFLECTANCE
 438 AS A MATURATION PARAMETER. *Organic Geochemistry*, 16, 313-323.
- 439 CASSANI, F., GALLANGO, O., TALUKDAR, S., VALLEJOS, C. & EHRMANN, U.
 440 1988. Methylphenanthrene maturity index of marine source rock extracts and
 441 crude oils from the Maracaibo Basin. *Organic Geochemistry*, 13, 73-80.
- 442 CORCORAN, D. & CLAYTON, G. 1999. INTERPRETATION OF VITRINITE
 443 REFLECTANCE PROFILES IN THE CENTRAL IRISH SEA AREA:
 444 IMPLICATIONS FOR THE TIMING OF ORGANIC MATURATION. *Journal of*
 445 *Petroleum Geology*, 22, 261-286.
- 446 DALLMANN, W. K. 1999. *Lithostratigraphic Lexicon of Svalbard*, Tromsø, Norsk
 447 Polarinstitut.
- 448 DIESSEL, C. F. K. & GAMMIDGE, L. 1998. Isometamorphic variations in the
 449 reflectance and fluorescence of vitrinite—a key to depositional environment.
 450 *International Journal of Coal Geology*, 36, 167-222.
- 451 ENGELHART, S. E., HORTON, B. P., NELSON, A. R., HAWKES, A. D., WITTER, R.
 452 C., WANG, K., WANG, P.-L. & VANE, C. H. 2013. Testing the use of microfossils
 453 to reconstruct great earthquakes at Cascadia. *Geology*.
- 454 HARLAND, W. B. 1997. Chapter 20 Paleogene history. *In: HARLAND, W. B. (ed.)*
 455 *Geological Society, London, Memoirs*. London: Geological Society, London.
- 456 HELLAND-HANSEN, W. 1992. Geometry and facies of Tertiary clinothem, Spitsbergen. *Sedimentology*, 39, 1013-1029.
- 457 MAJOR, H. & NAGY, J. 1972. *Geology of the Adventdalen map area*, Oslo, Norsk
 458 Polarinstitut.
- 460 MAKY, A. B. F. & RAMADAN, M. A. M. 2008. Nature of Organic Matter, Thermal
 461 Maturation and Hydrocarbon Potentiality of
 462 Khatatba Formation at East Abu-gharadig Basin, North Western Desert, Egypt.
 463 *Australian Journal of Basic and Applied Sciences*, 2, 194-209.
- 464 MANUM, S. B. & THRONDSSEN, T. 1978. Rank of coal and dispersed organic matter
 465 and its geological
 466 bearing in the Spitsbergen Tertiary. *Norsk Polarinstitut. Arbok*. Oslo.
- 467 MARSHALL, C. J. 2013. *Palaeogeographic development and economic potential of the*
 468 *coal-bearing palaeocene Todalen Member, Spitsbergen*. Thesis (Ph.D.), University
 469 of Nottingham.
- 470 ORHEIM, A., BIEG, G., BREKKE, T., HORSEIDE, V. & STENVOLD, J. 2007.
 471 Petrography and geochemical affinities of Spitsbergen Paleocene coals, Norway.
 472 *International Journal of Coal Geology*, 70, 116-136.
- 473 PAECH, H.-J. & KOCH, J. 2001. Coalification in Post-Caledonian Sediments on
 474 Spitsbergen. *In: TESSENHORN, F. (ed.) Intra-Continental Fold Belts CASE 1:*
 475 *West Spitsbergen*. Hannover: Geologisches Jahrbuch.

- 476 PETERS, K. E., WALTERS, C. C. & MOLDOWAN, J. M. 2005. *The Biomarker Guide*
477 *Volume 2: Biomarkers and Isotopes in Petroleum Exploration and Earth History.*
478 *Second Edition.*, Cambridge, Cambridge University Press.
- 479 PETERSEN, H. I. 2005. Oil Generation from coal source rocks: the influence of
480 depositional conditions and stratigraphic age. *Geological Survey of Denmark and*
481 *Greenland Bulletin*, 7, 9-12.
- 482 PETERSEN, H. I. & NYTOFT, H. P. 2006. Oil generation capacity of coals as a function
483 of coal age and aliphatic structure. *Organic Geochemistry*, 37, 558-583.
- 484 RADKE, M. 1988. Application of aromatic compounds as maturity indicators in source
485 rocks and crude oils. *Marine and Petroleum Geology*, 5, 224-236.
- 486 RADKE, M., WELTE, D. H. & WILLSCH, H. 1982. Geochemical study on a well in the
487 Western Canada Basin: relation of the aromatic distribution pattern to maturity
488 of organic matter. *Geochimica et Cosmochimica Acta*, 46, 1-10.
- 489 RADKE, M., WELTE, D. H. & WILLSCH, H. 1986. Maturity parameters based on
490 aromatic hydrocarbons: Influence of the organic matter type. *Organic*
491 *Geochemistry*, 10, 51-63.
- 492 RASMUSSEN, E. & FJELDSKAAR, W. 1996. Quantification of the Pliocene-Pleistocene
493 erosion of the Barents Sea from present-day bathymetry. *Global and Planetary*
494 *Change*, 12, 119-133.
- 495 STEPHENS, J. F., LEOW, H. M., GILBERT, T. D. & PHILP, R. P. 1985. Investigation of
496 the relationship between coal maturity and aromaticity: Characteristics of
497 sodium dichromate oxidation products of Australian vitrinite concentrates. *Fuel*,
498 64, 1537-1541.
- 499 TEICHMÜLLER, M. & DURAND, B. 1983. Fluorescence microscopical rank studies on
500 liptinites and vitrinites in peat and coals, and comparison with results of the
501 rock-eval pyrolysis. *International Journal of Coal Geology*, 2, 197-230.
- 502 TESSENHORN, F. 2001. *Intra-Continental Fold Belts CASE 1: West Spitsbergen*,
503 Hanover, Geologisches Jahrbuch.
- 504 THRONDSSEN, T. 1982. VITRINITE REFLECTANCE STUDIES OF COALS AND
505 DISPERSED ORGANIC MATTER IN TERTIARY DEPOSITS IN THE ADVENT-
506 DALEN AREA, SVALBARD. *Polar Research*, 1982, 77-91.
- 507 TISSOT, B. P., PELET, R. & UNGERER, P. 1987. Thermal history of sedimentary
508 basins, maturation indices, and kinetics of oil and gas generation. *AAPG*
509 *Bulletin*, 71, 1445-1466.
- 510 TRYGVASON ELIASSEN, G. 2014. *RE: Fieldwork Observations*. Type to MARSHALL,
511 C.
- 512
513
514
515
516
517
518
519
520
521
522
523
524
525
526
527

528 **Figure and Table Captions**

529

530 **All figures meant for colour online only**

531

532 **Table 1** – Vitrinite Reflectance (R_o), *n*-alkane, hopane, sterane and aromatic biomarker
 533 and maturity parameters within the Central Tertiary Basin coals. ^a after Cassani
 534 *et al.*, (1988), ^b after Radke *et al.*, (1982) *Pr/Ph* –pristane/phytane, $Pr/nC17 =$
 535 *Pristane/heptadecane* ratio, $CPI(1) = \frac{2(C_{23}+C_{25}+C_{27}+C_{29})}{(C_{22}+2(C_{24}+C_{26}+C_{28})+C_{30})}$,
 536 $TS/TM = 17\alpha\text{-}22,29,30\text{-trisorhopane} / 18\alpha\text{-}22,29,30\text{-}$
 537 *trisorhopane*, $TS/TH = \text{Total hopanes} / \text{Total steranes}$

538

539

540 **Table S1** –Vitrinite Reflectance (R_o) values and location for all sites used in this study

541

542 **Table S2** – Rock-Eval Pyrolysis results for all sites used in this study. T_{max} conversion
 543 to predicted R_o after *Teichmüller and Durand, 1983* and max burial depth
 544 calculated from vitrinite reflectance data after *Barker and Pawlewicz, 1994*

545

546

547

548 **Figure 1** – Map of the island of Spitsbergen showing the mines and settlements of the
 549 NW Central Tertiary Basin and sample locality and type.

550

551 **Figure 2** – The Van Mijenfjorden Group representing sedimentary infill of the Central
 552 Tertiary Basin, modified from Helland-Hansen (1992)

553

554 **Figure 3** – Comparison of the vitrinite reflectance profile in the Longyear Seam across
 555 Adventdalen from (A) BH4/2009 (B) Mine 7 Section (C) Bassen Field Section.
 556 Note the large variations seen in rank and the general trend to lower R_o % values
 557 upseam

558

559 **Figure 4** – Variation in rank (R_o) within the Longyear seam in Mine 7, Adventdalen.
 560 Examination of the distribution of vitrinite reflectance values measured shows a
 561 shift to lower values, bi-modal distribution upseam.

562

563 **Figure 5** – Comparison of the vitrinite reflectance profile in the Longyear Seam across
 564 Lunckefjellet from (A) BH 6A/2007 (B) BH 10/2007 (C) BH 15/2011 (D) BH
 565 10/2009. Note the large variations seen in rank and the general trend to lower
 566 R_o % values upseam

567

568 **Figure 6** – Variation in rank (R_o) within the Longyear seam in BH15-2011,
 569 Lunckefjellet. As in Adventdalen examination of the distribution of vitrinite
 570 reflectance values measured shows a shift to lower values, bi-modal distribution
 571 upseam.

572

573 **Figure 7** – Variation in hopane and *n*-alkane maturity parameters up-seam within the
 574 Longyear seam. Note little variation in maturity up-seam indicating no maturity gap.

575

576 **Figure 8** – Rock-Eval data from the Svalbard coals shows (A) HI vs R_o % shows that HI
 577 (oil potential exerts a strong control upon vitrinite reflectance in all areas studied
 578 N.B ash rich samples were removed as not representative and Lunckefjellet
 579 sample represents BH15/2011. (B) HI vs OI shows that the composition of the

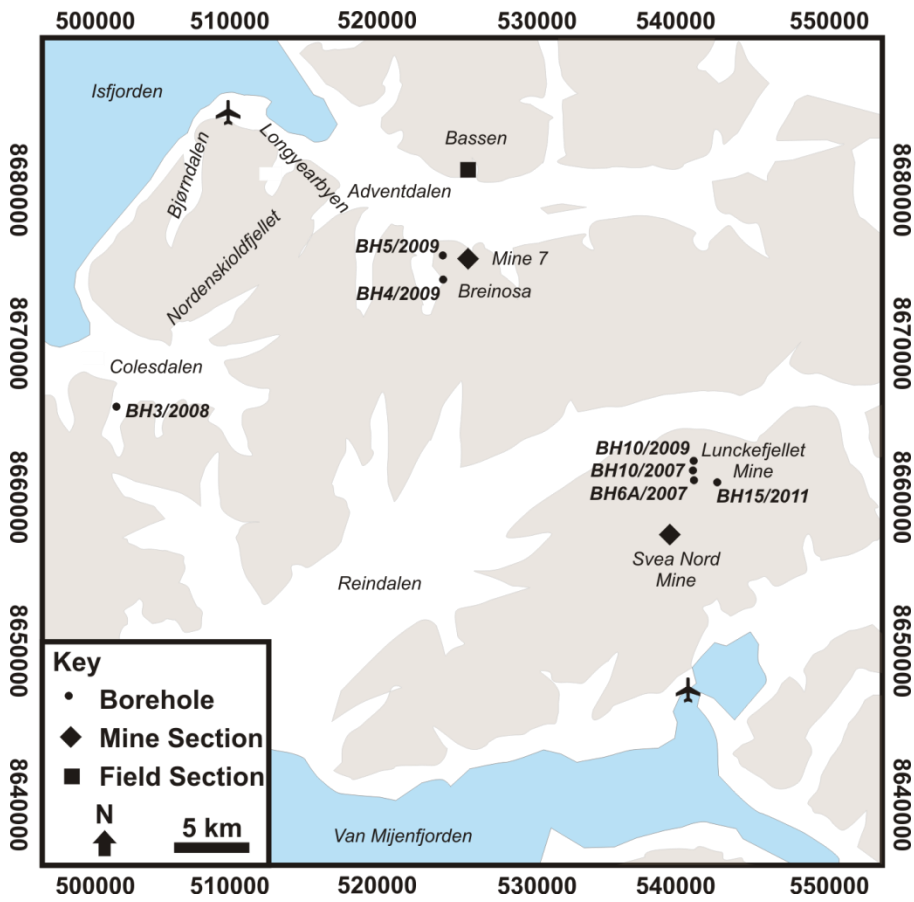
580 Svalbard coals is a cross between Type II and Type III kerogen with the
581 exception of Bassen Samples which has elevated OI values likely due to
582 weathering effects. (C) HI vs T_{max} and (D) HI vs. PI show that the Colesdalen
583 coals are most mature and closest to hydrocarbon generation with the least
584 mature coals found at Bassen. This is expected as Colesdalen is located in a
585 more central basinal position than Bassen at the basin margins.

586 **Figure 9** – Measurement of aromaticity of the Svalbard Coals of by ^{13}C NMR (A)
587 Longyear seam and (B) Svea seam. Note the large difference between the seam
588 indicating an apparent maturity equivalent to that of R0 0.5% and 0.78%
589 respectively (Carr and Williamson, 1990). This cannot be the case as the
590 Longyear is not a lignite, therefore the Longyear is enriched with non-coaly
591 aliphatics.

592
593
594
595
596
597
598
599
600
601
602
603
604
605
606
607
608
609
610
611
612
613
614
615
616
617
618
619
620
621
622
623
624
625
626
627
628
629
630
631

632
633
634
635
636
637
638

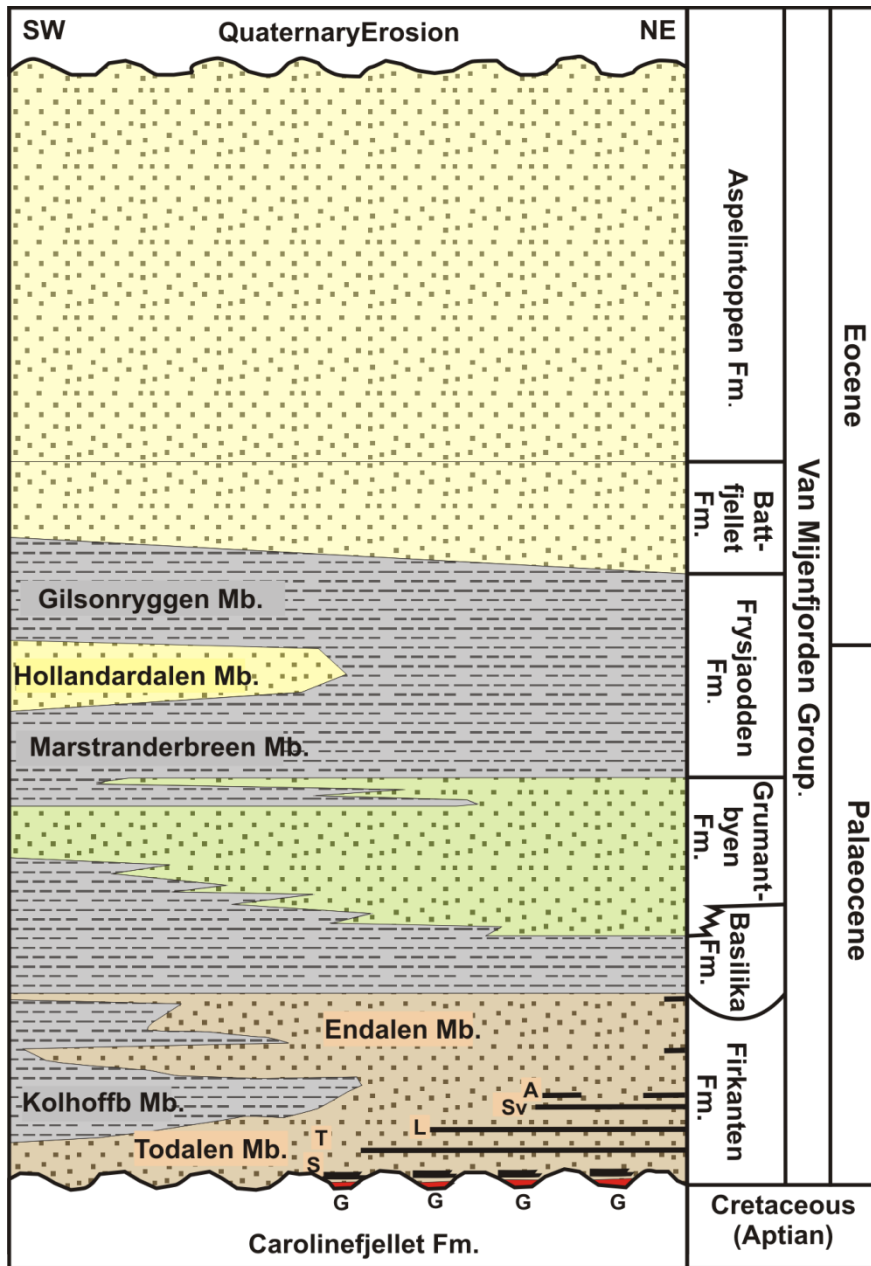
Figure 1



639
640
641
642
643
644
645
646
647
648
649
650
651
652
653
654
655
656
657
658
659

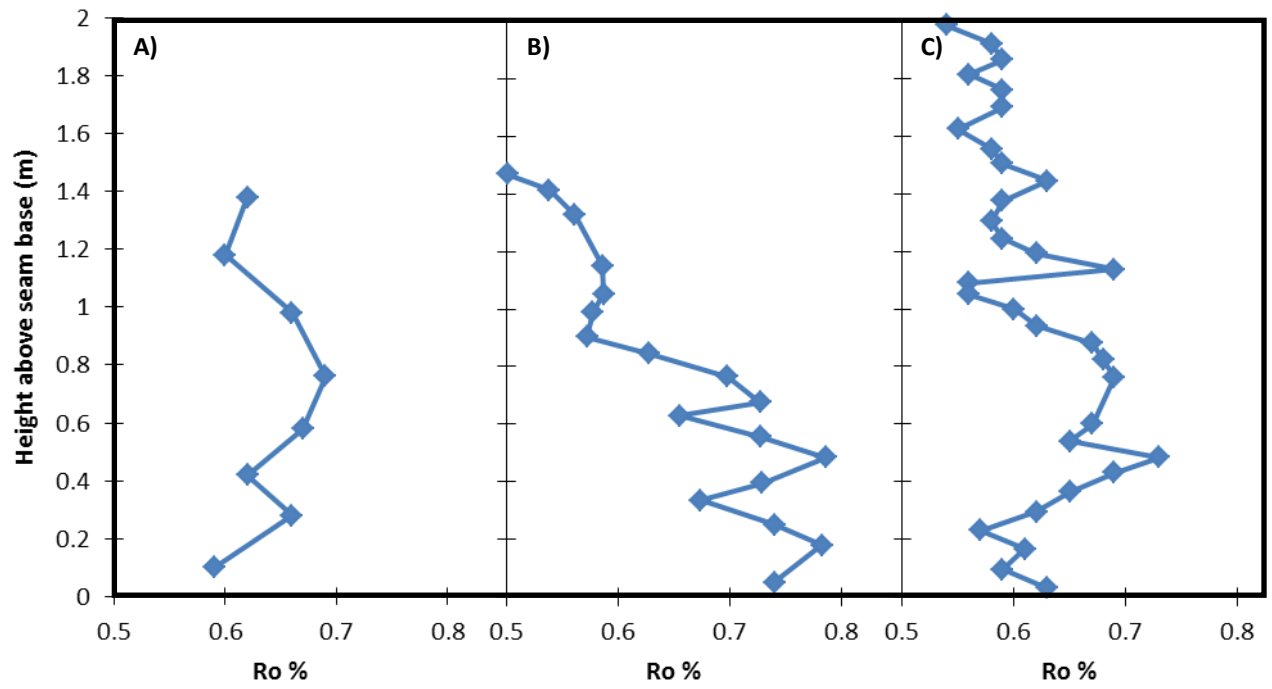
660
661
662
663

Figure 2



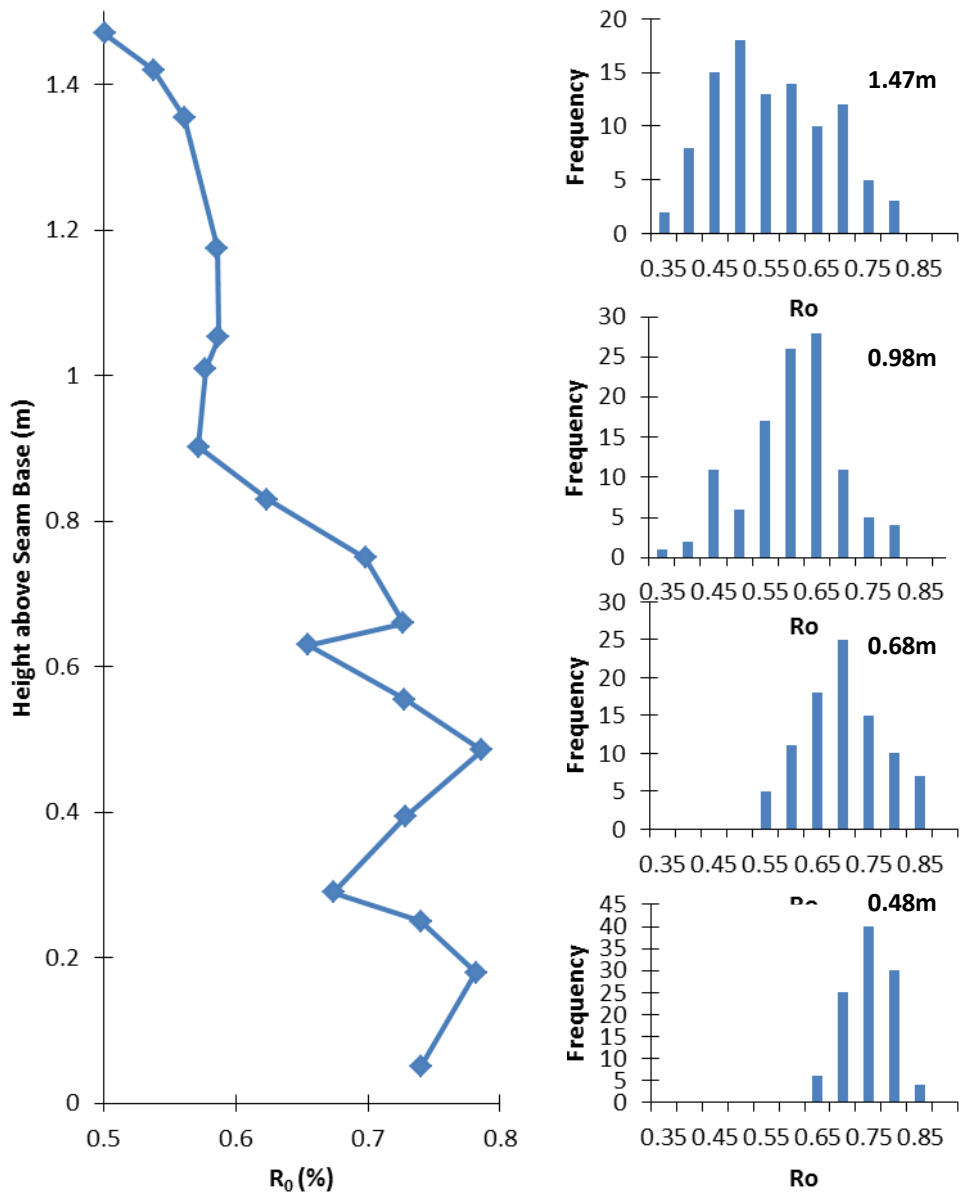
664
665
666
667
668
669
670
671
672
673
674
675
676

Figure 3



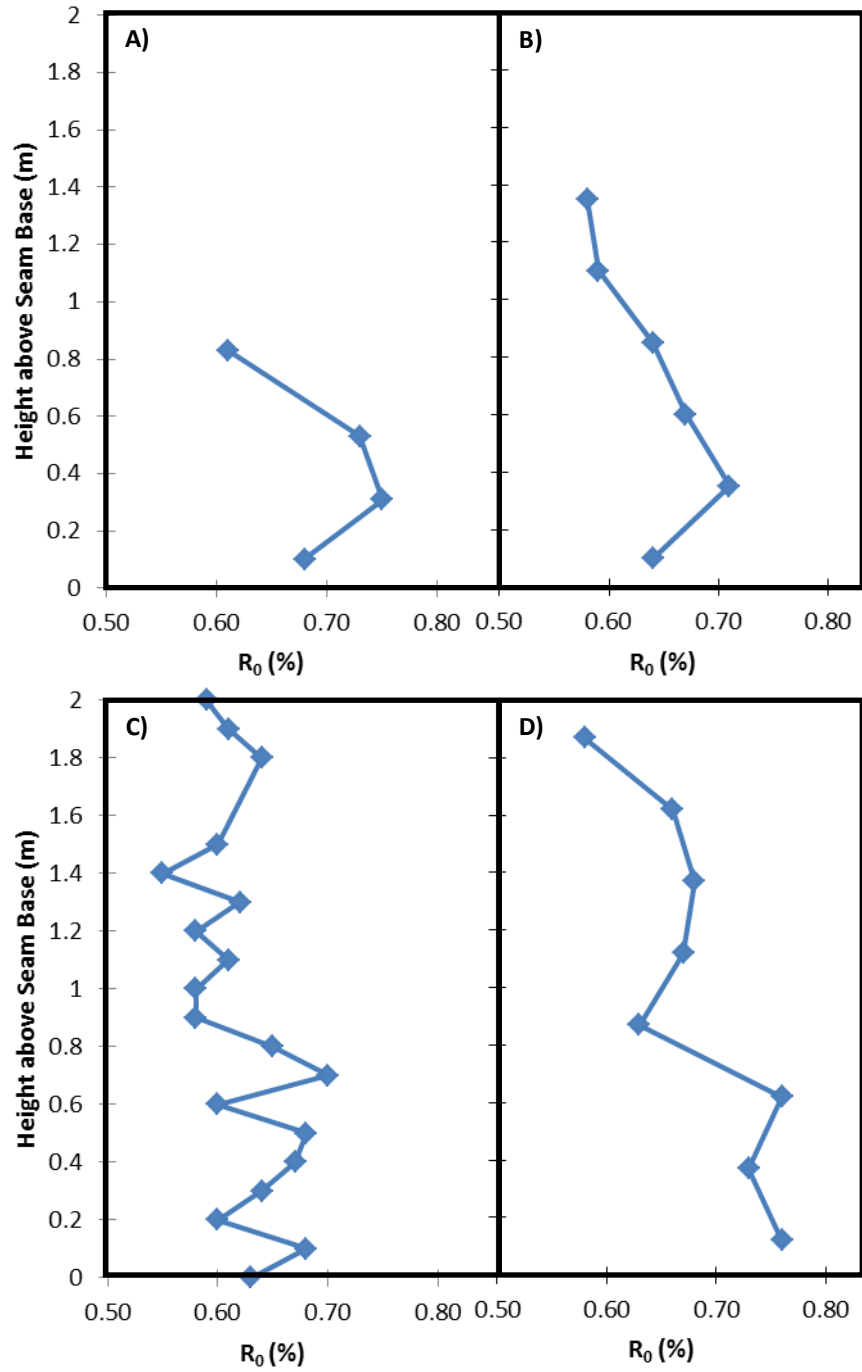
729 **Figure 4**

730
731
732
733
734
735
736
737
738
739
740
741
742
743
744
745
746
747
748
749
750
751
752
753
754
755
756
757
758
759
760
761
762
763
764
765
766
767
768
769
770
771
772
773
774
775
776
777
778
779
780



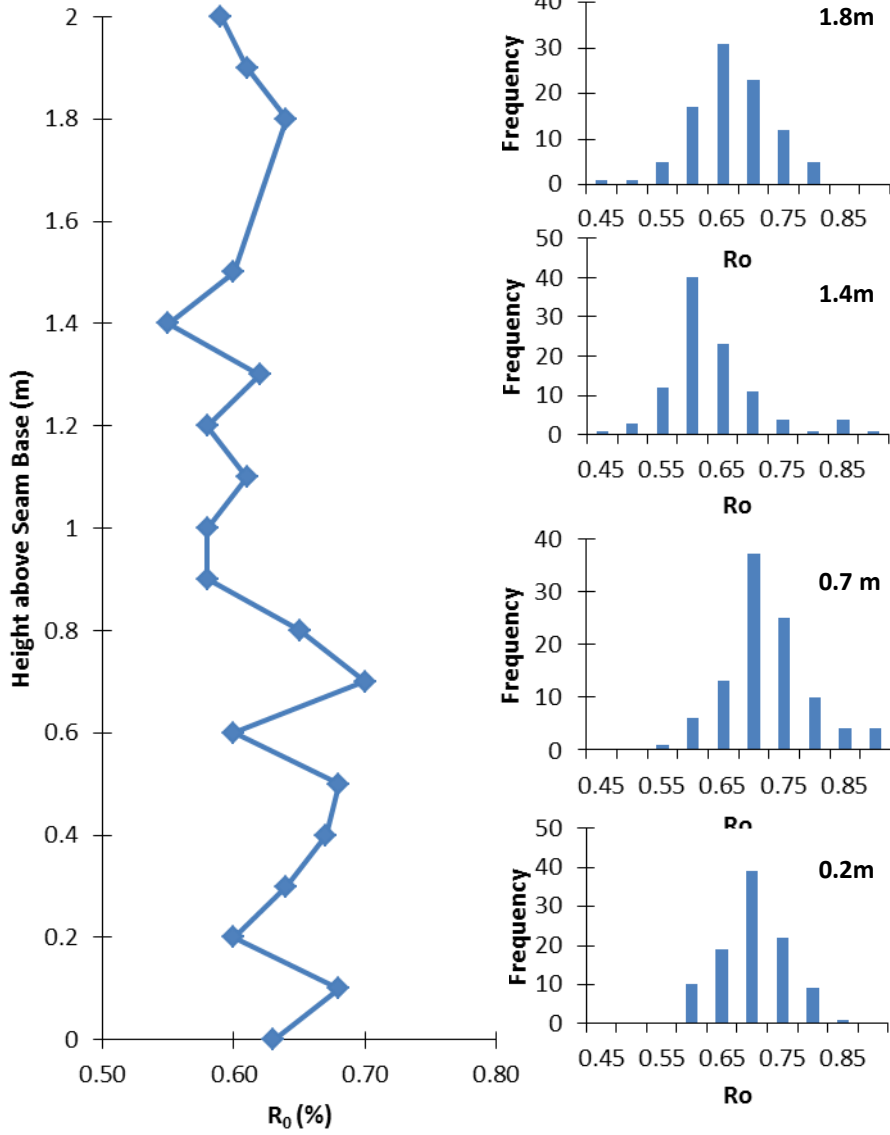
781 **Figure 5**

782
783
784
785
786
787
788
789
790
791
792
793
794
795
796
797
798
799
800
801
802
803
804
805
806
807
808
809
810
811
812
813
814
815
816
817
818
819
820
821
822
823
824
825
826
827
828
829
830
831
832

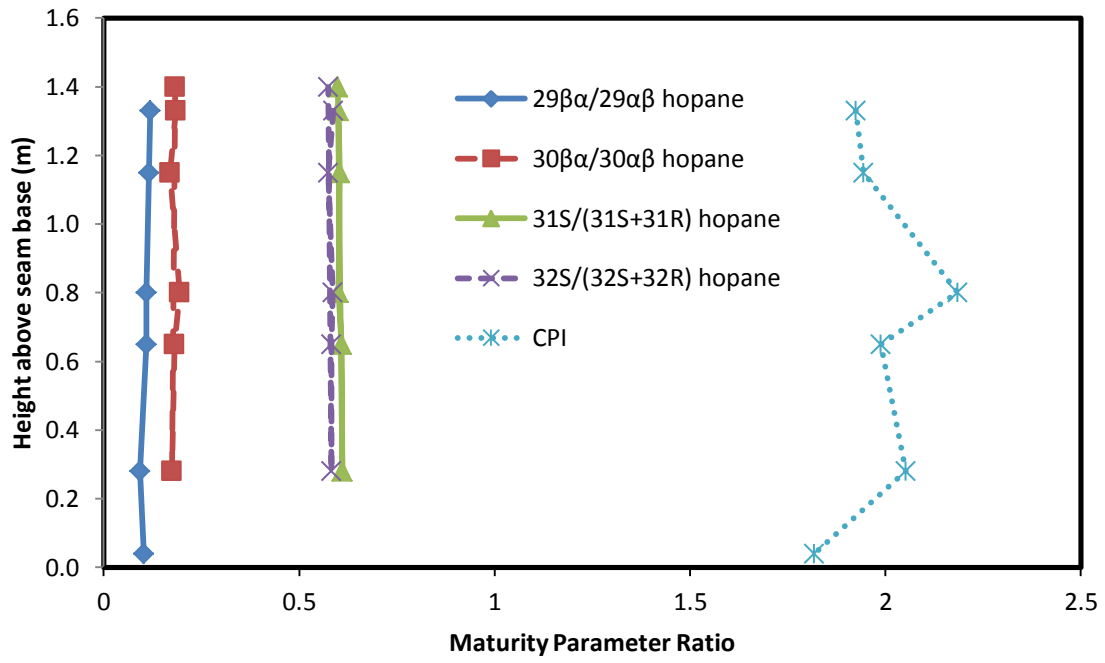


833 **Figure 6**

834
835
836
837
838
839
840
841
842
843
844
845
846
847
848
849
850
851
852
853
854
855
856
857
858
859
860
861
862
863
864
865
866
867
868
869
870
871
872
873
874
875
876
877
878
879
880
881
882
883
884

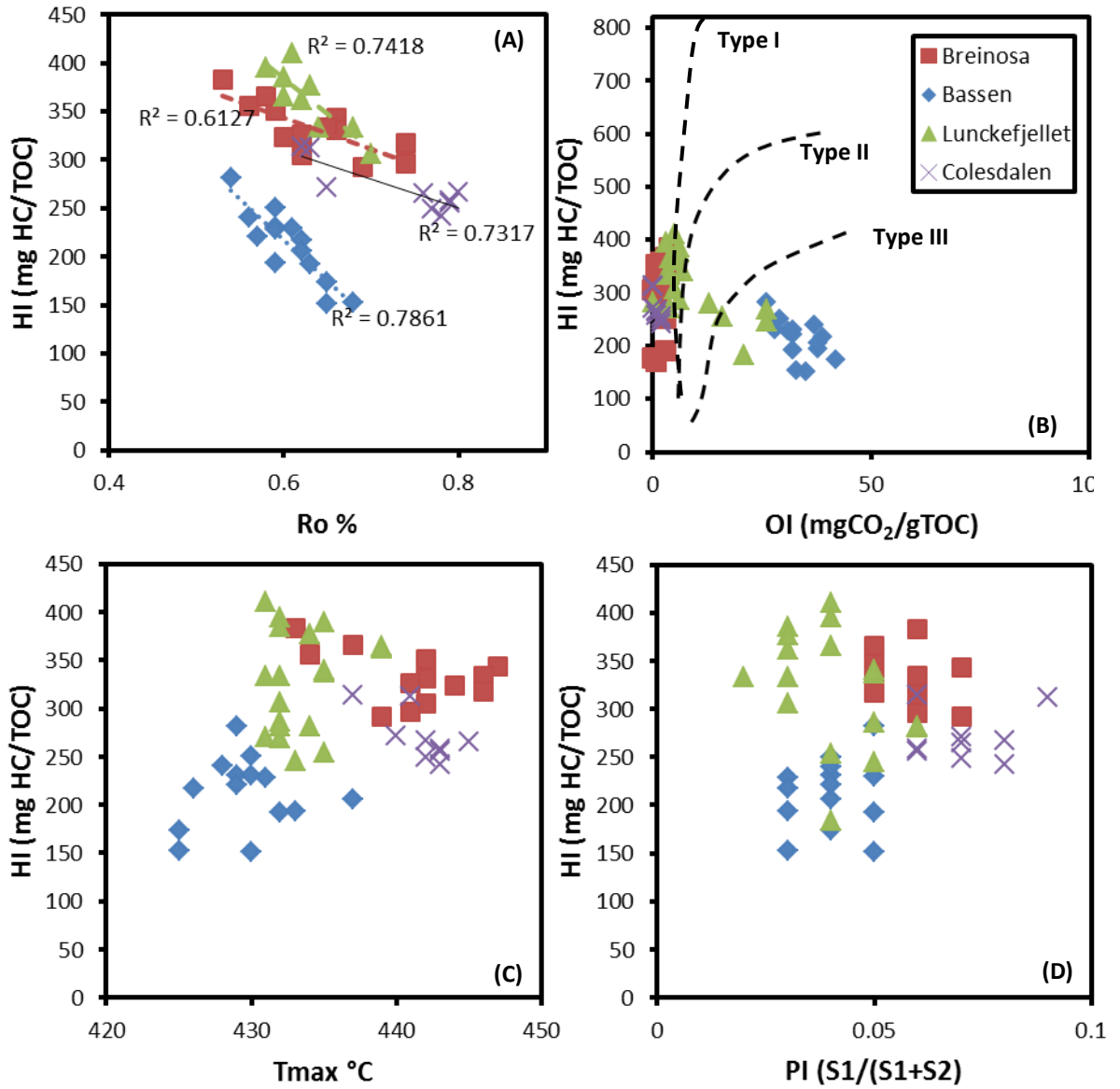


885 **Figure 7**
886
887

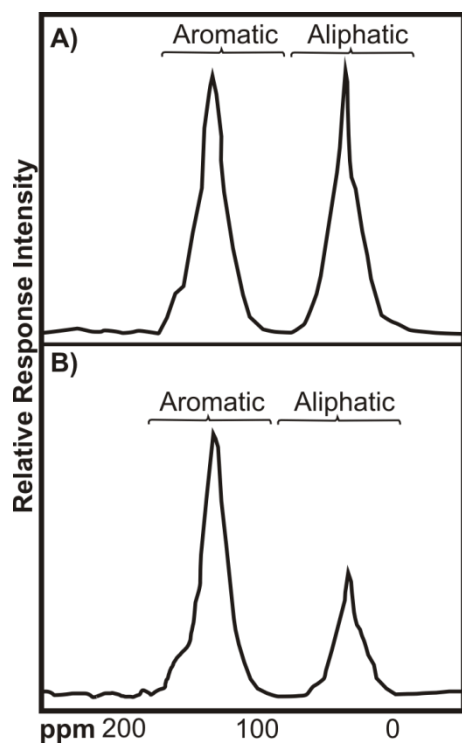


888
889
890
891
892
893
894
895
896
897
898
899
900
901
902
903
904
905
906
907
908
909
910
911
912
913
914
915
916
917
918

Figure 8



971 **Figure 9**
972



973
974
975
976
977
978
979
980
981
982
983
984
985
986
987
988
989
990
991
992
993
994
995
996
997
998
999
1000

1001
1002
1003**Table 1**

Seam	Seam Height (m)	R _o	Pr/Ph	Pr/nC ₁₇	Ph/nC ₁₈	CPI(1)	Ts/Tm	C ₂₉	C ₃₀	C ₃₁	C ₃₂	C ₃₃	C ₂₉ /C ₃₀	C ₃₅ /C ₃₄	C ₂₉	C ₂₉	TS/TH	MPI- ₁ ^a	Calculated R _o ^b
			n-alkanes				Hopanes						Sterane		Aromatic				
							βα/αβ	βα/αβ	S/(S+R)	S/(S+R)	S/(S+R)	αβ	αβ	S/S+R	β/α+β				
Svea Nord	Bulk	0.78	7.1	0.9	0.1	1.05	0.95	0.05	0.07	0.64	0.62	0.63	0.75	0.31	0.54	0.46	0.23	0.60	0.76
Longyear	Bulk	0.65	13.40	4.50	0.20	1.10	0.93	0.05	0.10	0.64	0.63	0.61	0.75	0.41	0.56	0.49	0.19	0.63	0.78
Svea Nord	0.07	0.77	4.48	24.55	4.43	1.46	0.93	0.09	0.08	0.58	0.58	0.58	0.58	0.43	0.42	0.51	0.21	0.48	0.69
Svea Nord	0.82	0.78	4.82	2.80	0.43	1.54	0.93	0.08	0.12	0.60	0.60	0.62	0.60	0.16	0.48	0.5	0.19	0.65	0.79
Breinosa Svea	0.75	0.78	3.51	22.48	3.77	1.41	0.94	0.07	0.09	0.59	0.59	0.62	0.63	0.23	0.51	0.51	0.19	0.51	0.71
Breinosa Svea	0.50	0.78	6.29	17.33	2.01	1.50	0.95	0.10	0.11	0.60	0.60	0.61	0.59	0.14	0.54	0.5	2	0.51	0.70
Breinosa Svea	1.00	0.79	3.53	2.70	0.66	1.54	0.93	0.08	0.09	0.62	0.62	0.64	0.56	-	0.47	0.53	0.2	0.49	0.69
Breinosa Svea	1.25	0.76	26.54	75.45	1.87	1.42	0.92	0.08	0.10	0.59	0.59	0.62	0.47	0.19	0.45	0.55	0.2	0.47	0.68
Todalen	-	0.75	20.99	119.83	2.93	1.39	0.93	0.06	0.07	0.60	0.60	0.63	0.55	0.28	0.47	0.49	0.21	0.57	0.74
Svarteper	0.73	0.65	3.01	0.68	0.27	1.40	0.91	0.10	0.05	0.58	0.58	0.59	0.50	-	0.48	0.52	0.2	0.76	0.86
Svarteper	0.94	0.65	6.49	9.99	0.97	1.57	0.95	0.09	0.13	0.60	0.60	0.61	0.61	0.16	0.49	0.51	0.21	0.56	0.74
Askeladden	0.33	0.64	2.95	6.23	1.73	1.39	0.94	0.11	0.10	0.59	0.59	0.62	0.54	0.29	0.48	0.5	0.21	0.52	0.71
Longyear	1.43	0.501	3.46	7.75	0.18	1.40	0.92	0.08	0.06	0.58	0.58	0.60	0.51	0.49	0.43	0.51	0.2	0.51	0.71
Longyear	1.43	0.538	11.44	12.22	1.34	1.59	0.93	0.11	0.07	0.60	0.59	0.60	0.67	0.30	0.45	0.49	0.18	0.51	0.71
Longyear	1.35	0.561	10.13	20.67	1.56	1.53	0.94	0.10	0.11	0.60	0.57	0.60	0.60	0.31	0.43	0.50	0.2	0.49	0.69
Longyear	1.17	0.586	11.41	17.37	1.15	1.56	0.95	0.09	0.12	0.60	0.59	0.62	0.62	0.30	0.45	0.50	0.21	0.55	0.73
Longyear	0.83	0.628	13.42	15.42	0.81	1.62	0.93	0.08	0.09	0.61	0.58	0.61	0.60	0.03	0.41	0.52	0.22	0.49	0.69
Longyear	0.66	0.655	12.11	5.29	0.33	1.69	0.93	0.08	0.10	0.61	0.58	0.60	0.62	0.41	0.41	0.52	0.23	0.55	0.73
Longyear	0.29	0.74	12.31	6.20	0.35	1.72	0.93	0.10	0.10	0.60	0.58	0.59	0.62	0.31	0.40	0.51	0.18	0.54	0.73
Longyear	0.07	0.74	13.60	2.34	0.16	1.69	0.94	0.11	0.12	0.60	0.57	0.61	0.63	0.31	0.42	0.51	0.19	0.45	0.67

1004